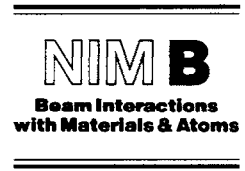




ELSEVIER



The interactions of high-energy, highly charged Xe ions with buckyballs

R. Ali ^a, H.G. Berry ^a, S. Cheng ^{a,1}, R.W. Dunford ^a, H. Esbensen ^a, D.S. Gemmell ^{a,*},
E.P. Kanter ^a, T. LeBrun ^a, L. Young ^a, W. Bauer ^b

^a Physics Division, Argonne National Laboratory, Argonne, IL 60439, USA

^b NSCL, Michigan State University, East Lansing, MI 48824, USA

Abstract

Ionization and fragmentation have been measured for C₆₀ molecules bombarded by highly charged (up to 35+) xenon ions with energies ranging up to 625 MeV. The observed mass distribution of positively charged fragments is explained in terms of a theoretical model indicating that the total interaction cross section contains roughly equal contributions from (a) excitation of the giant plasmon resonance, and (b) large-energy-transfer processes that lead to multiple fragmentation of the molecule. Preliminary results of measurements on VUV photons emitted in these interactions are also presented.

The relatively recent discovery [1] of the highly stable and symmetric quasi-spherical molecule C₆₀ and related fullerenes has led to intense studies on a wide variety of the properties of this new allotropic form of carbon. Research on these open cagelike structures (“buckyballs”) received a big boost when methods were developed [2] to produce them in macroscopic quantities.

An interesting aspect of the fullerenes is that they represent intermediate structures lying between the solid-state and the atomic scales. As is observed in the solid-state and in atomic (and indeed nuclear) systems, fullerenes also exhibit collective oscillations. This property is of fundamental importance in the measurements we report here and provides a direct link to this Symposium in honor of Rufus Ritchie who has contributed so much over the years to the development of the understanding of collective modes.

Among many approaches to the study of fullerenes, the use of atomic collision techniques offers a powerful tool for investigating their structures and their dynamics. Indeed several collision studies have already been reported [3]. Our experiments were performed at Argonne’s ATLAS heavy-ion linear accelerator, where we studied the interactions of high-energy (up to 625 MeV), highly charged (up to 35+) Xe ions with C₆₀. These beam energies exceeded those used in previous work by several orders of magnitude. The high values of projectile velocity and charge state result in excitation and decay processes differing

significantly from those seen in studies at lower energies (see, for example, Ref. [4]).

Our C₆₀ vapor target was formed from 99.5% pure material heated in an oven to 475°C. A time-of-flight (TOF) spectrometer system (see Fig. 1) was located at 90° to the incident beam. Grids around the target region were biased with voltages to extract positively charged fragments and to inject them into a 20 cm long gridded flight tube and thence into a microchannel plate detector. A “beam sweeper” at ATLAS was employed so as to allow one 0.4 ns wide beam pulse to reach the target every 10 μs. TOF spectra were obtained using a “multi-hit” time digitizer with the “start” signal coming from the detector and the “stop” signal from the accelerator’s timing system.

Fig. 2 shows the TOF spectrum and its equivalent calibration in terms of M/Q , the ratio of fragment mass to charge. The peaks in Fig. 2 that correspond to interactions of the projectiles with C₆₀ fall into three categories:

- (1) Peaks due to singly, doubly, triply, and (possibly) quadruply ionized C₆₀.
- (2) Peaks corresponding to the losses of even-numbered neutral carbon fragments.
- (3) Peaks corresponding to the sequence of singly charged fragments C_n⁺, with n assuming all values from 1 to at least 19. These peaks alternate in intensity up to around $n = 9$ with the odd-numbered peaks being more intense than the even-numbered. Above $n = 9$, the most intense peaks appear to be $n = 11, 15$, and probably 19. The intensity variations mirror those seen in other studies and indicate the relative stabilities of linear chain ($n \leq 9$) and cyclic ($n \geq 9$) structures. We refer to this series of peaks,

* Corresponding author.

¹ Present address: Dept. Physics and Astronomy, Univ. of Toledo, Toledo, OH 43615, USA.

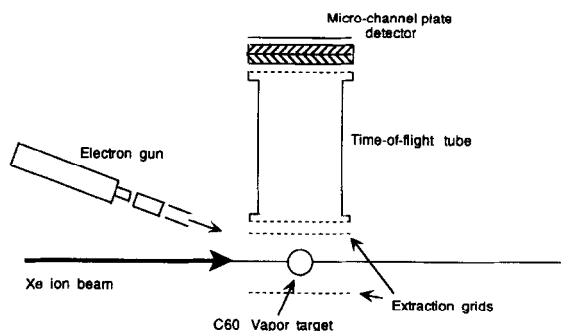


Fig. 1. Schematic diagram of experimental arrangement.

C_n^+ , as the “multifragmentation” peaks since they arise predominantly from events in which there is a catastrophic disintegration of the C_{60} molecule into many small fragments.

The manner in which energy is coupled into the C_{60} system from the passage of a highly charged fast ion (of velocity, v) depends strongly on the impact parameter. The two principal distances of importance are the mean radius, \bar{R} , (3.55 Å) of the C_{60} “cage” on which are located the nuclei of the constituent carbon atoms, and the adiabatic distance, $b_0 = \gamma \hbar v / E$ ($= 10$ Å for $E = 20$ eV), for the excitation of the giant dipole plasmon resonance of energy E . This collective excitation of the 240 valence electrons of the C_{60} molecule has been predicted [5–7] and measured [8–10] to have an energy of 20 eV and a FWHM of about 10 eV. As an interesting aside demonstrating the ubiquity of collective resonances at different scales, we show in Fig. 3 a comparison of the giant dipole resonances observed in the C_{60} molecule [9] and in the ^{12}C nucleus [11]. Note that the excitation-energy scales differ by a factor of approximately 10^6 .

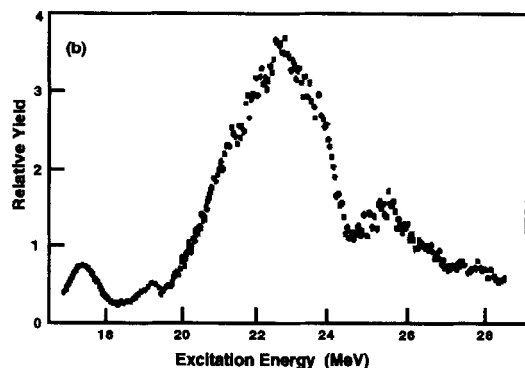
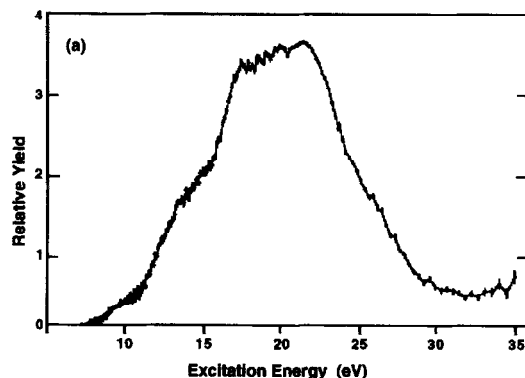


Fig. 3. Comparison of the giant dipole plasmon resonances observed in (a) the C_{60} molecule via photoionization with synchrotron radiation [9], and (b) the ^{12}C nucleus via the $^{11}\text{B}(p, \gamma)^{12}\text{C}$ reaction [11].

We have developed a quasi-classical model [12] for the interaction between projectile and buckyball that gives the total excitation and single-plasmon excitation probabilities

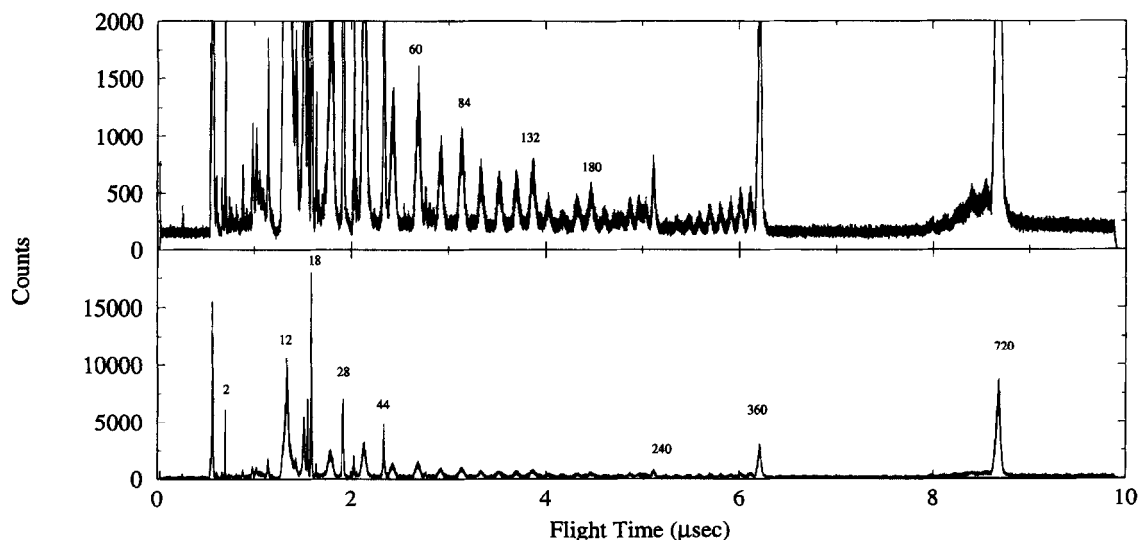


Fig. 2. Time-of-flight spectrum for positive fragments arising from bombardment of C_{60} by 625 MeV $^{136}\text{Xe}^{35+}$ ions. The numbers given above some of the peaks are the ratios (M/Q) of fragment mass (amu) to charge.

as a function of impact parameter. Preliminary to estimating the total interaction cross section, we consider the excitation of the giant dipole plasmon resonance by the Coulomb field of the xenon projectile. The effective number of plasmon excitations at an impact parameter b is

$$N(b) = \int dE \frac{f(E)}{E} \frac{2Z_p^2 e^4}{mv^2} \frac{1}{b^2} \times \left(\xi^2 K_1^2(\xi) + \frac{1}{\gamma^2} \xi^2 K_0^2(\xi) \right), \quad (1)$$

where $\xi = Eb/\gamma\hbar v$, $f(E)$ is the oscillator strength distribution, and Z_p is the charge state of the xenon ion. This expression, obtained in first-order perturbation theory, is consistent with that for the average energy transfer to a harmonic oscillator [13]. The predicted [5] oscillator strength is about 70. We have therefore parameterized the oscillator strength distribution $f(E)$ as a Gaussian, normalized to reproduce this and other known parameters of the resonance.

The excitation number $N(b)$ is large for $b \lesssim \bar{R}$. The strength of the plasmon resonance, combined with the high charge state of the xenon ion implies also that multiple excitations play an important role even at distances as big as the adiabatic distance, b_0 . To make a realistic estimate of cross sections, we describe the plasmon excitations in terms of a ‘‘coherent state’’ [14]. The multiplasmon excitation probabilities are then given by a Poisson distribution generated by $N(b)$. In particular, the probability for a one-plasmon excitation is $N(b) \exp(-N(b))$, and the total excitation probability is $1 - \exp(-N(b))$. These two probabilities are illustrated in Fig. 4a.

The total excitation probability reaches unity at an impact parameter of about 7 Å, still far outside the radius \bar{R} . To determine the total interaction cross section, it is therefore not necessary to consider explicitly reactions at the smaller impact parameters where the xenon ion may interact with individual electrons, and we can simply write this cross section as

$$\sigma_{\text{exc}} = 2\pi \int_0^\infty db b (1 - \exp(-N(b))). \quad (2)$$

The single-plasmon excitation cross section is

$$\sigma_{1\text{pl}} = 2\pi \int_0^\infty db b N(b) \exp(-N(b)). \quad (3)$$

This estimate is reasonable since all the cross section comes from impact parameters much larger than \bar{R} (cf. Fig. 4a). The total interaction cross section obtained from the calculated values shown in Fig. 4a is 811 Å², whereas the single-plasmon cross section is 387 Å², i.e. 48% of the total.

Our model should be valid for single-plasmon excitation involving large impact parameters where the linear response and dipole approximations hold. It can be expected to break down at smaller impact parameters where

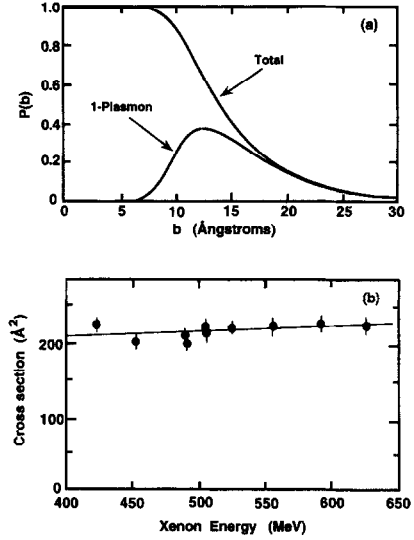


Fig. 4. (a) Calculated probabilities for the total interaction and for single-plasmon excitation as functions of the impact parameter, b , for 625 MeV $^{136}\text{Xe}^{35+}$ ions. (b) Calculated single-plasmon cross section (shown as a line) compared to the measured yields of C_{60}^+ from C_{60} bombarded by $^{136}\text{Xe}^{18+}$ ions in the energy range 420–625 MeV.

multiplasmon excitation occurs leading to multiple ionization, pair emission, and (at still smaller impact parameters) multifragmentation. The dominant decay mode of the single-plasmon excitation is thought to be via single-electron emission [9,15]. We therefore compare the calculated single-plasmon cross section (Eq. (3)) to our measured C_{60}^+ yield. The dependence on beam energy is illustrated in Fig. 4b for the projectile charge state $Z_p = 18$. The weak dependence on beam energy is reproduced by the calculation. We were unable to determine accurate experimental cross sections. However rough estimates based on the calculated vapor pressure, the integrated beam current, and taking into account the experimental geometry, detector efficiency, etc, agree with the calculated values within a factor of about 2. The slope of the calculated curve is insensitive to small variations in the total oscillator strength. We also considered the role of electron capture by the Xe ions as a production mechanism for C_{60}^+ ions but at the high velocities (11–14 a.u.) of our beams, the charge-capture cross sections [16] are negligible compared to the cross sections for plasmon excitation.

At impact parameters less than about 7 Å where the energy deposition becomes large, essentially all projectile/target interactions will result in multifragmentation. We have constructed a bond-percolation model [12] to describe these fragmentation processes. C_{60} is represented as a collection of lattice sites located at the positions of the carbon atoms. Each site is connected to its three nearest neighbors via bonds. We assume that each xenon ion deposits excitation energy in proportion to its pathlength

through the hollow fullerene structure. The energy is then rapidly distributed in a uniform manner over the whole C_{60} cluster. This leads to the breaking of individual bonds with a probability proportional to the total energy deposition, which in turn, is dependent on the impact parameter. The fragment-mass distribution calculated using this model compares well with the measured fragment mass spectrum (Fig. 5).

Although the giant dipole resonance is known to decay overwhelmingly by single-electron emission [9,15] there should exist a relatively small ($\sim 10^{-4}$ to 10^{-5}) photon decay branch. We calculated that we ought to be able to observe this decay and so we set up a VUV diffraction grating spectrometer at 90° to the incident beam direction looking for photons in the 20 eV range. For these measurements the maximum ion beam current (“unswept”) and charge state were employed. After getting the background radiation down to acceptable levels, we found that the VUV spectrum in the region of interest (from ~ 400 to ~ 1300 Å) was dominated by photons emitted from (mostly) singly charged carbon ions (C II). We were therefore unable to identify photons from the giant resonance. A typical spectrum is shown in Fig. 6. The measured peaks in terms of the photon energies and relative intensities agree well with those determined in earlier work with gaseous discharges [17].

The electron configurations involved in the observed VUV transitions shown in Fig. 6 are all in the valence shells of C II. These transitions are known [17] to have short (< 1 ns) lifetimes. In our measurements we measured the lifetimes of the transitions relative to the arrival time of the beam pulse at the target. All of them displayed these expected short lifetimes, but interestingly, some of them, e.g. the 687 Å and the unresolved (806 + 809) Å transitions shown in Fig. 6, exhibit also significant long-lived components on the order of 100 ns. These long-lived components presumably reflect the production lifetimes for

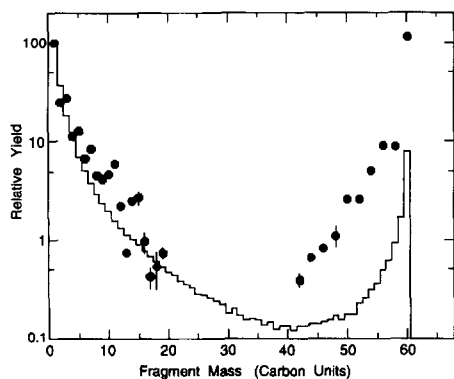


Fig. 5. Measured mass distribution (solid points) for positive fragments arising from C_{60} bombarded by 625 MeV $^{136}\text{Xe}^{35+}$ ions. The histogram is the distribution calculated on the basis of a multifragmentation model.

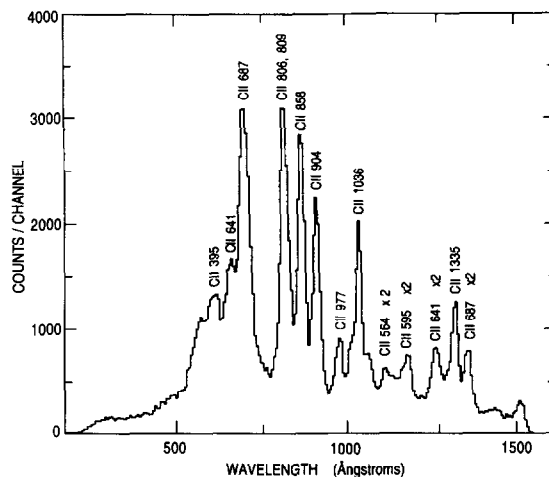


Fig. 6. VUV photon spectrum measured with a position-sensitive detector at the focal plane of a grating spectrometer located perpendicular to the incident beam direction. The xenon projectile energy was 625 MeV and the average charge state (after foil stripping just upstream of the C_{60} target) was $40+$. The peaks are labelled with identifications derived from the tabulations given in Ref. [17].

these particular configurations of C II in the interaction of a xenon ion with C_{60} . We are currently trying to understand in more detail how these configurations arise and to see if they are connected in any direct way with the original bonding in the target molecule.

Acknowledgement

This work was supported by the US Department of Energy, Office of Basic Energy Sciences, Contract W-31-109-ENG-38. We wish to thank B.J. Zabransky and C.A. Kurtz for their invaluable technical assistance.

Note added in proof

Some of the material presented here was also presented at the 7th Int. Conf. on the Physics of Highly Charged Ions, Vienna, Austria, 1994 (Nucl. Instr. and Meth. B 98 (1995) 479).

References

- [1] H.W. Kroto, J.R. Heath, S.C. O'Brien, R.F. Curl and R.E. Smalley, *Nature* 318 (1985) 162.
- [2] W. Krätschmer, L.D. Lamb, K. Fostiropoulos and D.R. Huffman, *Nature* 347 (1990) 354.
- [3] For reviews see e.g.: E.E.B. Campbell et al., *Nuclear Physics*

- Concepts in Atomic Cluster Physics, (Springer, Berlin, 1992) and Proc. 18th Int. Conf. on the Physics of Electronic and Atomic Collisions, Aarhus, Denmark, 1993.
- [4] B. Walch, C.L. Cocke, R. Voelpel and E. Salzborn, Phys. Rev. Lett. 72 (1994) 1439.
- [5] G.F. Bertsch, A. Bulgac, D. Tomanek and Y. Wang, Phys. Rev. Lett. 67 (1991) 2690.
- [6] G. Barton and C. Eberlein, J. Chem. Phys. 95 (1991) 1512.
- [7] D. Östling, P. Apell and A. Rosén, Europhys. Lett. 21 (1993) 539.
- [8] R.K. Yoo, B. Ruscic and J. Berkowitz, J. Chem. Phys. 96 (1992) 911.
- [9] I.V. Hertel, H. Steger, J. deVries, B. Weisser, C. Menzel, B. Kamke and W. Kamke, Phys. Rev. Lett. 68 (1992) 784.
- [10] J.W. Keller and M.A. Coplan, Chem. Phys. Lett. 193 (1992) 89.
- [11] R.G. Allas, S.S. Hanna, L. Meyer-Schützmeister and R.E. Segel, Nucl. Phys. 58 (1964) 122.
- [12] T. LeBrun, H.G. Berry, S. Cheng, R.W. Dunford, H. Esbensen, D.S. Gemmell and E.P. Kanter, Phys. Rev. Lett. 72 (1994) 3965.
- [13] J.D. Jackson, Classical Electrodynamics (Wiley, New York, 1962).
- [14] See e.g.: E. Merzbacher, Quantum Mechanics (Wiley, New York, 1970).
- [15] T. Drewello, W. Krätschmer, M. Fieber-Erdman and A. Ding, Int. J. Mass Spectrosc. and Ion Proc. 124 (1993) R1.
- [16] A.S. Schlachter, J.W. Stearns, W.G. Graham, K.H. Berkner, R.V. Pyle and J.A. Tanis, Phys. Rev. A 27 (1983) 3372.
- [17] R.L. Kelly and L.J. Palumbo, Atomic and Ionic Emission Lines below 2000 Å (NRL Report 7599. US Govt. Printing Office, Washington DC, 1973).